Journal of
Marine Science and Engineering

MDPI

Article

Neural Network Identification-Based Model Predictive Heading Control for Wave Gliders

Peng Jin, Baolin Zhang * and Yun Zhang

College of Automation and Electronic Engineering, Qingdao University of Science & Technology, Qingdao 266061, China; 2022040006@mails.qust.edu.cn (P.J.); zhangyun@qust.edu.cn (Y.Z.)
* Correspondence: zhangbl2020@qust.edu.cn

Abstract: This paper deals with the neural network identification-based model predictive heading control problem in a wave glider. First, based on a kinematic model of the wave glider subjected to external disturbance and system uncertainty, a state space model of the wave glider is established. Then, a neural network identification-based model predictive heading controller (NNI-MPHC) is designed for the wave glider. The heading controller mainly includes three components: a model predictive controller, a neural network-based model identifier, and a linear reduced-order extended state observer. Third, a design algorithm of the NNI-MPHC is presented. The algorithm is demonstrated through simulation, where the results show the following: (i) The designed NNI-MPHC is remarkably capable of guaranteeing the tracing effects of the wave glider. (ii) Comparing the NNI-MPHC and existing heading controllers, the former is better than the latter in terms of tracking accuracy and rapidity and robustness to model uncertainty and/or external disturbances.

Keywords: wave glider; model predictive control; neural network identification; heading control; extended state observer

Citation: Jin, P.; Zhang, B.; Zhang, Y. Neural Network Identification-Based Model Predictive Heading Control for Wave Gliders. *J. Mar. Sci. Eng.* **2024**, *12*, 2279. https://doi.org/10.3390/jmse12122279

Academic Editor: Rafael Morales

Received: 19 November 2024
Revised: 6 December 2024
Accepted: 7 December 2024
Published: 11 December 2024

1. Introduction

The modeling, navigation, and control of unmanned vehicles in ocean environments, such as autonomous underwater vehicles and surface craft, have attracted an increasing amount of attention in recent decades (see [1–6], and the references therein). In particular, the wave glider, a novel type of unmanned surface vehicle, has garnered significant interest. In fact, owing to their small size, light weight, and lack of fuel propulsion, wave gliders are well suited for long-duration, long-range reconnaissance, and detection missions [3]. However, wave gliders present significant challenges for practical applications in modeling and navigation due to their complex dynamics, which include a nonlinear, time-varying, underactuated, and double-body structured system. For instance, the yaw angle of wave glider is categorized into two components: glider yaw angle and float yaw angle. Using only one of these components as the heading angle can result in suboptimal control performance. To address this situation, a heading fusion method was proposed for wave gliders in [7], where the yaw angles of the float and the glider are considered jointly to obtain a merged heading angle. Additionally, in [8,9], a dynamic model of the wave glider was introduced that accounts for the tension, relaxation, and time-delay effects of the umbilical cable, alongside a Kalman filter algorithm to predict system states under variable structural conditions.

To effectively deal with the navigation challenges faced by wave gliders, it is essential to design appropriate heading control schemes, such as active disturbance rejection control (ADRC) [10,11] and sliding mode control [12–14]. To mitigate the impact of significant perturbations, an ADRC-based approach was developed, which integrates an S-surface control algorithm and a linear extended state observer to enhance performance [10]. Additionally, to reduce overshoot caused by excessive control actions in complex marine environments, in [11], an improved anti-windup algorithm and a reduced-order extended

state observer were introduced. The impact of marine bio-pollution on the physical properties of lightweight unmanned vehicles, such as wave gliders, cannot be overlooked. Addressing this concern, in [15], an adaptive sliding mode heading control scheme was proposed to manage the uncertainties within the wave glider model.

Since the wave glider's propulsion cannot be autonomously controlled, its heading control system, along with dynamic position-keeping algorithms, plays a crucial role in enhancing spotting operations [16]. The application of ambient forces to the surrounding environment has been shown to improve the precision of position-keeping control. To this end, the weather optimal positioning control (WOPC) system has been implemented [17]. As underdriven systems, the ability to control the trajectory of wave gliders is a crucial aspect of their operation. However, in practice, due to the inherent uncertainty in the speed at which wave gliders navigate through waves, traditional line-of-sight (LOS) algorithms encounter challenges in accurately tracking their position, resulting in instances of overshooting or slow convergence. To address this issue, an adaptive LOS algorithm was proposed, which contains the ability to dynamically adjust in the look-head distance [1]. For a wave glider with a propeller–rudder system, a predictive LOS system was designed for the better utilization of steering characteristics [18]. To ensure safe navigation and obstacle avoidance, a kinematically constrained safe rapidly-exploring random tree (RRT) path planning algorithm was introduced to solve the path planning problem in wave gliders [19].

Note that accurately modeling the wave glider's dynamics to solve heading control problems presents a significant challenge. Furthermore, most existing heading control algorithms for wave gliders are primarily focused on the rejection of disturbance and the design of the extended state observer, often neglecting the inherent structural properties of the wave glider. As a result, performance metrics related to heading control, such as tracking accuracy and system robustness of the wave glider, are not satisfied. This raises an important question that how to effectively utilize the limited structural information of wave glider to develop robust heading control schemes. Addressing this challenge is the primary motivation of the present study. Fortunately, model predictive control (MPC) is well suited for handling complex disturbances in marine environments due to its unique predictive and rolling optimization capabilities [20,21]. When combined with a neural network identifier for real-time model identification, MPC can effectively address the nonparametric disturbances resulting from time-varying dynamic of the wave glider [22]. In this paper, we simultaneously employ a model predictive algorithm, a neural network identification method [23], and a reduced-order extended state observer design scheme [24] to develop a novel heading controller for the wave glider. The main contributions of this paper are outlined as follows:

- An NNI-based model predictive heading controller (NNI-MPHC) is developed for wave gliders, where only the system order of a glider is required, the system parameters can be identified online, and a reduced-order extended state observer is designed to estimate the unmodeled dynamics and unknown disturbance.
- Simulation results show that the designed NNI-MPHC is effective at tracking the predefined input of the wave glider. In addition, the NNI-MPHC outperforms the existing heading controllers of wave gliders with respect to the accuracy and rapidity of tracking and the robustness to the model uncertainty and/or external disturbances.

In the rest of this paper, Section 2 presents the state space model and formulates heading control problems in wave gliders. Section 3 provides the detailed design scheme of the NNI-MPHC. Section 4 presents simulation results and illustrates the effectiveness and advantages of the designed heading controller, and Section 5 summarizes the main conclusions of this paper.

2. Problem Formulation

As illustrated in Figure 1, the wave glider consists of three main components: a submerged float, an underwater glider, and an umbilical cable that interconnects them.

Currently, there are two types of wave glider models. The first one is the unitary model, which encompasses the surge, sway, pitch, and roll motions of the entire wave glider, as well as the yaw movements of float and glider, resulting in a total of six degrees of freedom [25–27]. The second model is a simplified version, which focusing solely on the relationship between the input rudder angle and the yaw motion of the wave glider [8,9,28]. To investigate the heading control design problem in wave gliders, this paper adopts the second, simplified model. The following assumptions are necessary to present the kinematic model of the wave glider [11]:

Assumption 1. *The pitch and roll of the wave glider are regarded as the disturbances.*

Assumption 2. *The umbilical cable is always in tension and the glider is of high quality enough, the difference between the heading angles of the float and the glider can be ignored.*

Assumption 3. *The rudder angle is regarded as the control input of the wave glider.*

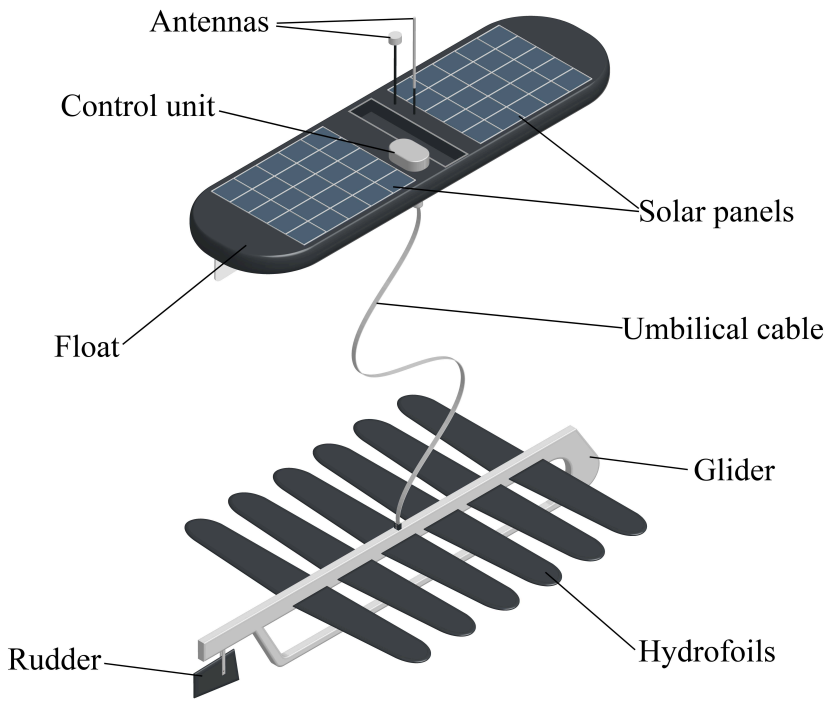

Figure 1. The overall structure of a wave glider.

By considering the motion coordinate system shown in Figure 2 and the low-speed characteristics of the wave glider, a kinematic model of the glider can be expressed as [10,29]:

$$[T_w(t) + \Delta T_w]\ddot{\varphi}(t) + [\alpha(t) + \Delta\alpha]\dot{\varphi}(t) + [\beta(t) + \Delta\beta]\dot{\varphi}^3(t) = [K_w(t) + \Delta K_w][\delta(t) + \delta_d(t)] \quad (1)$$

where $\varphi(t)$ and $\delta(t)$ are the heading angle and the rudder angle of the wave glider, respectively. $\delta_d(t)$ is the external disturbance, ΔT_w, $\Delta\alpha$, $\Delta\beta$, and ΔK_w are the model uncertainties, and

$$K_w(t) = \frac{K_0 U(t)}{U_0},\ T_w(t) = \frac{T_0 U_0}{U(t)},\ \alpha(t) = \alpha_0\left[\frac{U_0}{U(t)}\right]^2,\ \beta(t) = \beta_0\left[\frac{U_0}{U(t)}\right]^2 \quad (2)$$

where $U(t)$ is the speed of glider, K_0, T_0, U_0, α_0, and β_0 are known constants.

Let

$$\bar{x}_1(t) = \varphi(t),\ \bar{x}_2(t) = \dot{\varphi}(t)$$

and

$$d_m(t) = -\Delta T_w(t)\dot{\bar{x}}_2(t) - \Delta\alpha\bar{x}_2(t) - \Delta\beta\bar{x}_2^3(t) + \Delta K_w\delta_d(t) \tag{3}$$

Then, from (2), one yields the state space model of the wave glider as follows:

$$\dot{\bar{x}}(t) = \bar{\boldsymbol{A}}(t)\bar{\boldsymbol{x}}(t) + \bar{\boldsymbol{B}}(t)\delta(t) + \bar{\boldsymbol{E}}(t)f(\bar{\boldsymbol{x}}) + \bar{\boldsymbol{B}}(t)d_e(t) + \bar{\boldsymbol{E}}_m(t)d_m(t) \tag{4}$$

where $d_e(t) = \delta_d(t),\ f(\bar{\boldsymbol{x}}) = \bar{x}_2^3(t)$, and

$$\bar{\boldsymbol{x}}(t) = \begin{bmatrix}\bar{x}_1(t)\\ \bar{x}_2(t)\end{bmatrix},\ \bar{\boldsymbol{A}}(t) = \begin{bmatrix}0 & 1\\ 0 & -\dfrac{\alpha(t)}{T_w(t)}\end{bmatrix},\ \bar{\boldsymbol{B}}(t) = \begin{bmatrix}0\\ \dfrac{K_w(t)}{T_w(t)}\end{bmatrix},$$

$$\bar{\boldsymbol{E}}(t) = \begin{bmatrix}0\\ -\dfrac{\beta(t)}{T_w(t)}\end{bmatrix},\ \bar{\boldsymbol{E}}_{\boldsymbol{m}}(t) = \begin{bmatrix}0\\ \dfrac{1}{T_w(t)}\end{bmatrix}$$

The yaw angle is selected as the output variable, i.e., the output equation of the system is in the form

$$\bar{y}(t) = \bar{\boldsymbol{C}}\bar{\boldsymbol{x}}(t) \tag{5}$$

where $\bar{\boldsymbol{C}} = [1\ \ 0]$.

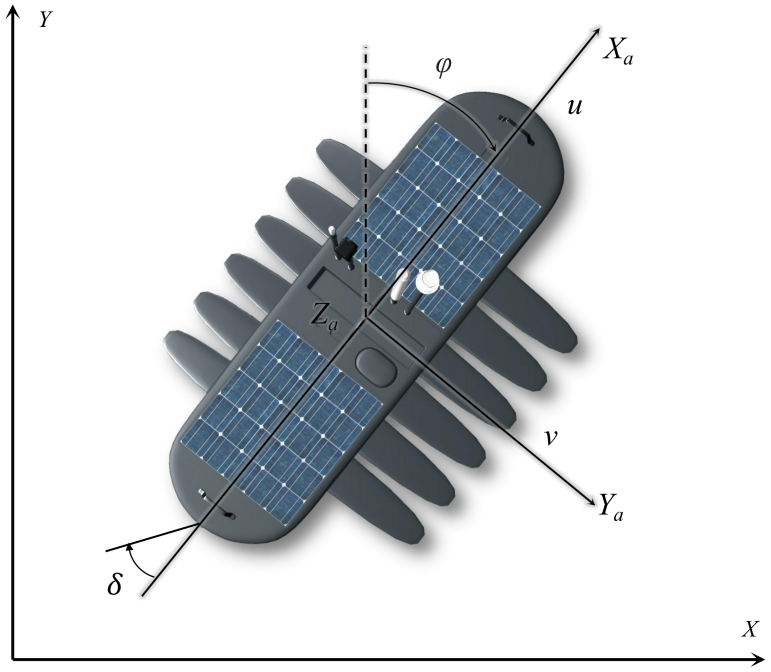

Figure 2. Motion coordinate system for a wave glider [30].

3. Heading Controller Design of Wave Glider

In this section, for the wave glider system (4), one presents in detail a neural network identification-based model predictive heading controller. As shown in Figure 3, the system structure mainly includes a model predictive controller (MPC), a neural network-based identifier (NNI), and a linear reduced-order extended state observer (LRESO).

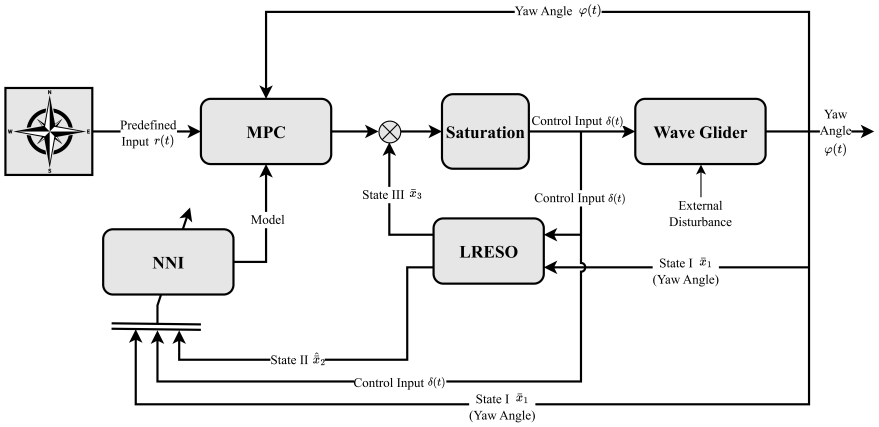

Figure 3. The overall structure of NNI-MPHC.

3.1. Design of the LRESO

In the wave glider system, the yaw angle state $\bar{x}_1(t)$ can be directly measured, while the second state $\bar{x}_2(t)$ is unknown. To obtain the state $\bar{x}_2(t)$, there are several observers that can be used, such as the Romberg observer [31], the sliding mode observer [32], and the extended state observer [33]. In this paper, an LRESO is introduced as [24]

$$\begin{cases} \dot{z}_2(t) = z_3(t) + \beta_{02}\bar{x}_1(t) + b\delta(t) - \beta_{01}(z_2(t) + \beta_{01}\bar{x}_1(t)) \\ \dot{z}_3(t) = -\beta_{02}(z_2(t) + \beta_{01}\bar{x}_1(t)) \end{cases} \tag{6}$$

and the estimates of $\bar{x}_2(t)$ and the extended state $\bar{x}_3(t)$ are

$$\begin{cases} \hat{\bar{x}}_2(t) = z_2(t) + \beta_{01}\bar{x}_1(t) \\ \bar{x}_3(t) = z_3(t) + \beta_{02}\bar{x}_1(t) \end{cases} \tag{7}$$

where β_{01}, β_{02}, and b are the constants of LRESO. Moreover, the control input becomes

$$\delta(t) = \text{sat}\left(\delta_0 - \frac{\bar{x}_3(t)}{b}\right) \tag{8}$$

where δ_0 is the control output of the MPC, and $\text{sat}(\cdot)$ is the saturation function.

Remark 1. *Since the first state of the observer can be directly measured, only the second state needs to be estimated. In comparison to the linear extended state observer [10] and the fuzzy mode-dependent state switched fuzzy observer [34], the proposed LRESO in this paper can reduce the phase lag, and it is more simple and convenient to realize in practical applications.*

3.2. Design of NNI

To design a neural network-based identifier for the wave glider, a Hopfield network with six neurons is selected in this paper. The interconnectivity of neurons is a fundamental attribute of Hopfield networks, which do not necessitate pre-training as a prerequisite for functionality. Therefore, it is specifically suitable for the identification problem of systems with time-varying parameters. The input–output relation can be described as [35]

$$\begin{cases} C_i\dfrac{du_i}{dt} = \displaystyle\sum_{j=1}^{n}\omega_{ij}v_j - \frac{u_i}{R_i} + I_i \\ v_i = g(u_i) \end{cases} \tag{9}$$

and the detailed structure of Hopfield network is presented in Figure 4 and the hyperbolic function $g(\cdot)$ can be expressed as

$$g(x) = \frac{\rho(1 - e^{-\lambda x})}{1 + e^{-\lambda x}} \tag{10}$$

where $i = 1, 2, \cdots, n$, R_i and C_i are the resistance and inductance values of the amplifier, u_i is the unamplified voltage value, v_i is the amplified voltage value which simultaneously implies the output of each neuron in the neural network, I_i is the external excitation signal, ω_{ij} is the corresponding connection weight, and ρ and λ are constants.

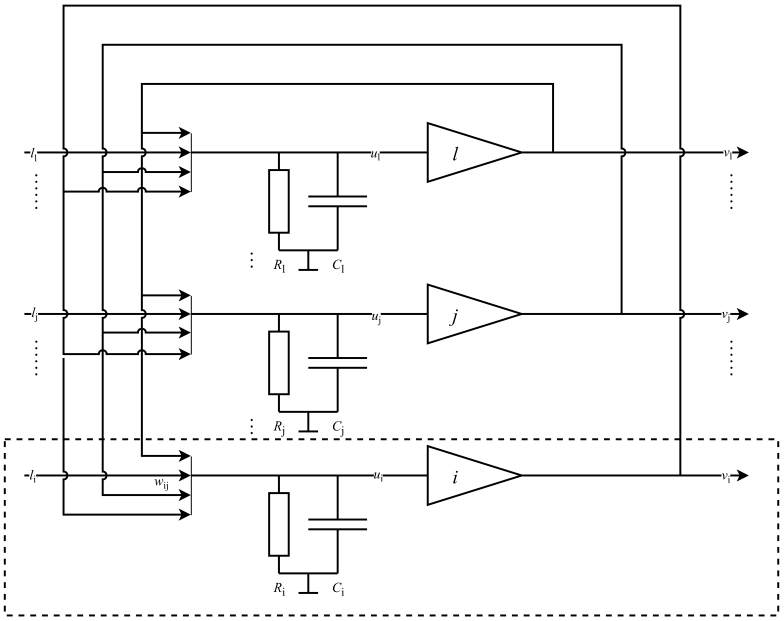

Figure 4. The overall structure of Hopfield network.

By ignoring the external disturbance and model uncertainties to linearize the wave glider system (4) and replacing the unknown states with the estimated ones via (6), one obtains a local linear model of wave glider as

$$\dot{\hat{\bar{x}}}(t) = \bar{A}(t)\hat{\bar{x}}(t) + \bar{B}(t)\delta(t) \tag{11}$$

where $\hat{\bar{x}}(t)$ is the estimated value of the second state $\bar{x}(t)$ as

$$\hat{\bar{x}}(t) = \begin{bmatrix} \bar{x}_1(t) \\ z_2(t) + \beta_{01}\bar{x}_1(t) \end{bmatrix} = \begin{bmatrix} \bar{x}_1(t) \\ \hat{\bar{x}}_2(t) \end{bmatrix}$$

Suppose that the identified model of the system (11) is in the form of

$$\dot{\boldsymbol{x}}_p(t) = \hat{\boldsymbol{A}}(t)\hat{\bar{\boldsymbol{x}}}(t) + \hat{\boldsymbol{B}}(t)\delta(t) \tag{12}$$

where $\hat{A}(t)$ and $\hat{B}(t)$ are defined as

$$\hat{\boldsymbol{A}}(t) = \begin{bmatrix} a_{11}(t) & a_{12}(t) \\ a_{21}(t) & a_{22}(t) \end{bmatrix}, \ \hat{\boldsymbol{B}}(t) = \begin{bmatrix} b_1(t) \\ b_2(t) \end{bmatrix}$$

where $a_{ij}(t)$ and $b_i(t)$ denote the time-varying parameters to be identified.

Let $\boldsymbol{e}_{id}(t) = \hat{\bar{\boldsymbol{x}}}(t) - \boldsymbol{x}_p(t)$. Then, from (11) and (12), one obtains

$$\dot{\boldsymbol{e}}_{id}(t) = [\bar{\boldsymbol{A}}(t) - \hat{\boldsymbol{A}}(t)]\hat{\bar{\boldsymbol{x}}}(t) + [\bar{\boldsymbol{B}}(t) - \hat{\boldsymbol{B}}(t)]\delta(t) \tag{13}$$

Define

$$E_{id} = \frac{1}{2}\dot{\boldsymbol{e}}_{id}^{T}\dot{\boldsymbol{e}}_{id} \tag{14}$$

and suppose that the amplifiers are ideal, that is, in (9), $R_i \to \infty$ and $C_i = 1$. Then, a Hopfield network standard energy function can be introduced as [35]

$$E_h = -\frac{1}{2}\sum_i\sum_j \omega_{ij}\nu_i\nu_j - \sum_i I_i\nu_i \tag{15}$$

Define $\boldsymbol{W} = (\omega_{ij}) \in \mathbb{R}^{i\times j}$, $\boldsymbol{F} = (I_i) \in \mathbb{R}^{i\times 1}$, and $\boldsymbol{V} = (\nu_i) \in \mathbb{R}^{i\times 1}$. Let

$$\boldsymbol{V}(t) = \begin{bmatrix} a_{11}(t) & a_{12}(t) & a_{21}(t) & a_{22}(t) & b_1(t) & b_2(t) \end{bmatrix}^T$$

Then, from (14) and (15), one obtains

$$\boldsymbol{W}(t) = -\begin{bmatrix} \bar{x}_1 & \bar{x}_1\hat{\bar{x}}_2 & 0 & 0 & \bar{x}_1\delta & 0 \\ \hat{\bar{x}}_2\bar{x}_1 & \hat{\bar{x}}_2^2 & 0 & 0 & \hat{\bar{x}}_2\delta & 0 \\ 0 & 0 & \bar{x}_1^2 & \bar{x}_1\hat{\bar{x}}_2 & 0 & \bar{x}_1\delta \\ 0 & 0 & \hat{\bar{x}}_2\bar{x}_1 & \hat{\bar{x}}_2^2 & 0 & \hat{\bar{x}}_2\delta \\ \delta\bar{x}_1 & \delta\hat{\bar{x}}_2 & 0 & 0 & \delta^2 & 0 \\ 0 & 0 & \delta\bar{x}_1 & \delta\hat{\bar{x}}_2 & 0 & \delta^2 \end{bmatrix}, \ \boldsymbol{F}(t) = \begin{bmatrix} \bar{x}_1\dot{\bar{x}}_1 \\ \hat{\bar{x}}_2\dot{\bar{x}}_1 \\ \bar{x}_1\dot{\hat{\bar{x}}}_2 \\ \bar{x}_2\dot{\hat{\bar{x}}}_2 \\ \delta\dot{\bar{x}}_1 \\ \delta\dot{\hat{\bar{x}}}_2 \end{bmatrix} \tag{16}$$

Further, from (9) and (16), one can obtain the identification results $\boldsymbol{V}$. Notice that in practice, the nonlinear term $f(\bar{\boldsymbol{x}})$, the external disturbance term $d_e(t)$, and the model uncertainty perturbation $d_m(t)$ always exist, which means the identified parameters $\hat{\boldsymbol{A}}(t)$ and $\hat{\boldsymbol{B}}(t)$ are always biased.

3.3. Design of MPC

Based on the parameter identification results in Section 3.2, one yields a local linear model of the wave glider as

$$\begin{cases} \dot{\hat{\bar{\boldsymbol{x}}}}(t) = \hat{\boldsymbol{A}}(t)\hat{\bar{\boldsymbol{x}}}(t) + \hat{\boldsymbol{B}}(t)\delta_0(t) \\ \bar{y}(t) = \bar{\boldsymbol{C}}\hat{\bar{\boldsymbol{x}}}(t) \end{cases} \tag{17}$$

where $\delta_0(t)$ is the control output of the MPC. To apply the MPC, by using the zero-order holding method, discretize the above continuous system as

$$\boldsymbol{x}(k+1) = \boldsymbol{A}(k)\boldsymbol{x}(k) + \boldsymbol{B}(k)\delta_0(k) \tag{18}$$

where

$$\boldsymbol{A}(k) \triangleq \Phi((k+1)T, kT), \ \boldsymbol{B}(k) \triangleq \int_{kT}^{(k+1)T} \Phi((k+1)T, \tau)\mathrm{d}\tau\hat{\boldsymbol{B}}(kT) \tag{19}$$

with T the sample period, $\Phi(\cdot,\cdot)$ the state transition matrix of system (17).

The corresponding output vector can be expressed as

$$y(k) = \boldsymbol{C}\boldsymbol{x}(k) \tag{20}$$

where $\boldsymbol{C} = \bar{\boldsymbol{C}}$.

Let

$$\Delta\boldsymbol{x}(k) = \boldsymbol{x}(k) - \boldsymbol{x}(k-1), \ \Delta\delta_0(k) = \delta_0(k) - \delta_0(k-1) \tag{21}$$

Then, from (18) and (20), one obtains

$$\begin{cases} \Delta\boldsymbol{x}(k+1) = \boldsymbol{A}\Delta\boldsymbol{x}(k) + \boldsymbol{B}\Delta\delta_0(k), \\ y(k) = \boldsymbol{C}\Delta\boldsymbol{x}(k) + y(k-1) \end{cases} \tag{22}$$

Suppose that $\delta_0(k)$ and $\Delta\delta_0(k)$ satisfy the following constraints:

$$\delta_{\min} \le \delta_0(k) \le \delta_{\max}, \quad \Delta\delta_{\min} \le \Delta\delta_0(k) \le \Delta\delta_{\max} \tag{23}$$

where $\delta_{\min}, \delta_{\max}, \Delta\delta_{\min}$, and $\Delta\delta_{\max}$ are known constants.

Introduce the cost function $\boldsymbol{J}$ as

$$\boldsymbol{J} = \sum_{i=1}^{n} Q\tilde{e}^2(k,i) + \sum_{i=0}^{m-1} R\delta_0^2(k+i \mid k) \tag{24}$$

where $\tilde{e}(k,i) = y(k+i \mid k) - r(k)$, Q and R are weight coefficients, n is the prediction horizon, m is the control horizon, $y(k+i \mid k)$ and $\delta_0(k+i \mid k)$ represent the predicted values, and $r(k)$ is a predefined input.

The predictive function can be expressed as [36]

$$\boldsymbol{Y_k} = \boldsymbol{M}\Delta\boldsymbol{x}(k) + \boldsymbol{I}y(k) + \boldsymbol{H}\Delta\boldsymbol{U_k} \tag{25}$$

where $\boldsymbol{Y_k} \in \mathbb{R}^{n\times 1}, \Delta\boldsymbol{U_k} \in \mathbb{R}^{m\times 1}, \boldsymbol{M} \in \mathbb{R}^{n\times 2}, \boldsymbol{I} \in \mathbb{R}^{n\times 1}, \boldsymbol{H} \in \mathbb{R}^{n\times m}$, and

$$\boldsymbol{Y_k} = \begin{bmatrix} y(k+1 \mid k) \\ y(k+2 \mid k) \\ \vdots \\ y(k+n \mid k) \end{bmatrix}, \ \Delta\boldsymbol{U_k} = \begin{bmatrix} \Delta\delta_0(k+0 \mid k) \\ \Delta\delta_0(k+1 \mid k) \\ \vdots \\ \Delta\delta_0(k+m-1 \mid k) \end{bmatrix}, \ \boldsymbol{M} = \begin{bmatrix} \boldsymbol{CA} \\ \boldsymbol{CA}^2 + \boldsymbol{CA} \\ \vdots \\ \sum_{i=1}^{n} \boldsymbol{CA}^i \end{bmatrix},$$

$$\boldsymbol{I} = \begin{bmatrix} 1 \\ 1 \\ \vdots \\ 1 \end{bmatrix}, \ \boldsymbol{H} = \begin{bmatrix} \boldsymbol{CB} & \boldsymbol{0} & \cdots & \boldsymbol{0} \\ \boldsymbol{CAB} + \boldsymbol{CB} & \boldsymbol{CB} & \cdots & \boldsymbol{0} \\ \vdots & \vdots & \ddots & \vdots \\ \sum\limits_{i=1}^{n} \boldsymbol{CA}^{i-1}\boldsymbol{B} & \sum\limits_{i=1}^{n-1} \boldsymbol{CA}^{i-1}\boldsymbol{B} & \cdots & \sum\limits_{i=1}^{n-m+1} \boldsymbol{CA}^{i-1}\boldsymbol{B} \end{bmatrix}$$

Then, define

$$\boldsymbol{P_k} = \boldsymbol{R_m} - \boldsymbol{M}\Delta\boldsymbol{x}(k) - \boldsymbol{I}y(k) \tag{26}$$

where $\boldsymbol{R_m} = [r(k+1) \ r(k+2) \ \cdots \ r(k+n)]^T$ is the predefined input sequence.

From (24), (25), and (26), the cost function J can be rewritten as

$$\boldsymbol{J} = \Delta\boldsymbol{U_k}^T L_1 \Delta\boldsymbol{U_k} - L_2\Delta\boldsymbol{U_k} \tag{27}$$

where

$$L_1 = \boldsymbol{H}^T Q^2 \boldsymbol{H} + R^2, \ L_2 = 2\boldsymbol{H}^T Q^2 \boldsymbol{P_k}$$

Note that by taking the control constraints and output constraints (23) into account, the optimization problem of constraints MPC can be transformed into solving a quadratic programming problem [36]. Solving the above quadratic programming problem, the MPC-based heading controller of the wave glider can be determined.

Remark 2. *Note that the proposed NNI-MPHC consists of three key components: a neural network-based model identifier, a linear reduced-order extended state observer, and a model predictive controller. The model identifier generates a more accurate and simplified time-varying linear model of the unmanned sailboat. The extended state observer makes the design of heading controller simple and physically realizable, and the model predictive scheme is introduced such that the heading control performance of the unmanned sailboat is optimized in whole given continuous time intervals. Compared to the existing heading controllers for unmanned sailboat, the NNI-MPHC is expected to deliver improved accuracy, faster response, and enhanced system robustness, which will be demonstrated through simulations.*

Now, the design algorithm of NNI-MPHC is outlined in Algorithm 1.

Algorithm 1 An algorithm of NNI-MPHC

Input: Predefined input $r(t)$, speed of wave glider $U(t)$
Output: Heading angle of wave glider $\varphi(t)$
Set Simulation time t_f
Set parameters: $Q, R, n, m, \rho, \lambda, \beta_{01}, \beta_{02}, b_0$
Initialization: network output $\boldsymbol{V}(0)$, wave glider states $U(0), x(0), \delta(0)$
while $t \leq t_f$ **do**
    $\hat{\boldsymbol{A}}(t), \hat{\boldsymbol{B}}(t) \Leftarrow \boldsymbol{V}(t)$
    Update $\boldsymbol{A}(t), \boldsymbol{B}(t), \boldsymbol{C}$ on (19) and (20)
    Update $\Delta \boldsymbol{x}(k), \Delta\delta(k)$ on (21)
    $\boldsymbol{J} \Leftarrow \boldsymbol{A}(t), \boldsymbol{B}(t), \boldsymbol{C}, \Delta \boldsymbol{x}(k), \Delta\delta(k), y(k), r(k)$
    Update $\delta_0(t)$ by solving $\boldsymbol{J}$
    $\delta(t) \Leftarrow \text{sat}[\delta_0(t) + \bar{\boldsymbol{x}}_3(t)]$
    Update $\bar{\boldsymbol{x}}(t)$ on (4)
    Update $\hat{\bar{\boldsymbol{x}}}_2(t)$ and $\bar{\boldsymbol{x}}_3(t)$ on (6)
    Update $\boldsymbol{W}(t)$ and $\boldsymbol{F}(t)$ on (16)
    Update $\boldsymbol{V}(t)$ on (9)
end while

4. Simulation Results

4.1. Parameters of the Wave Glider

To verify the effectiveness and advantage of the designed heading controller NNI-MPHC, an example wave glider is adopted , and system parameters are taken from [37]; the main values of system parameters in (2) are listed in Table 1. Suppose that the speed of the wave glider $U \in [0, 1.5]$ m/s, the control input $\delta(t)$, i.e., the flapping angle of the wave glider ranges from $-40°$ to $40°$. The initial values of control input, speed, and yaw angle of glider are set as $\delta(0) = 0°, U(0) = 0.4$ m/s, and $\varphi(0) = 0°$.

Table 1. Parameter values of a wave glider.

Parameter	Value	Parameter	Value
K_0	0.02	U_0	0.15
T_0	1.5	α_0	10
β_0	1		

In (4), suppose that the external disturbance term $d_e(t)$ is approximated by a colored noise ranging from $[-15°, 15°]$, which is shown in Figure 5. Due to the difficulty in determining the exact form of model uncertainty, the wave glider's model uncertainty is empirically defined as follows

$$d_m(t) = 2\sin(0.3\bar{x}_1(t)\hat{x}_2(t)),\ 0 \leq t \leq 600 \text{ s} \tag{28}$$

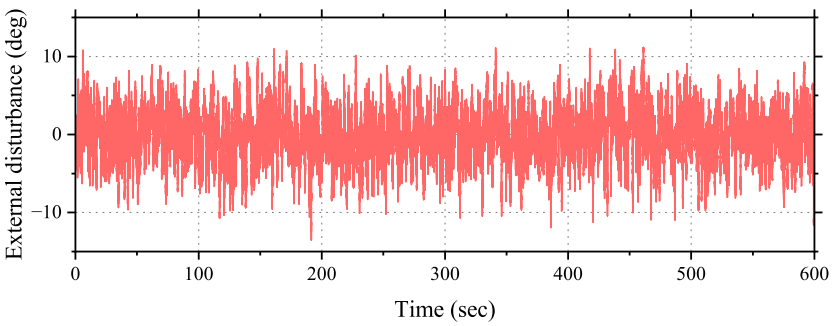

Figure 5. External disturbance added in wave glider.

The predefined input $r(t)$ is respectively simulated by a constant function $r_s(t)$ and a time-varying function $r_c(t)$, where

$$r_s(t) = \begin{cases} 30°, & 0\ \text{s} \le \text{t} < 200\ \text{s} \\ -20°, & 200\ \text{s} \le \text{t} < 400\ \text{s} \\ 15°, & 400\ \text{s} \le \text{t} \le 600\ \text{s} \end{cases} \tag{29}$$

and

$$r_c(t) = \begin{cases} 20\cos(0.03t), & 0\ \text{s} \le \text{t} < 300\ \text{s} \\ \text{Constant}, & 300\ \text{s} \le \text{t} \le 600\ \text{s} \end{cases} \tag{30}$$

In what follows, as shown in Table 2, given three different cases regarding the predefined input $r(t)$, external disturbance $d_e(t)$, and model uncertainty $d_m(t)$, the NNI-MPHC is designed and applied to the wave glider to show the heading control effects.

Table 2. Three cases of $r(t)$, $d_e(t)$, and $d_m(t)$.

Cases	$r(t)$	$d_e(t)$	$d_m(t)$
I	$r_s(t)$ in (29)	See Figure 5	0
II	$r_c(t)$ in (30)		0
III	$r_c(t)$ in (30)		See (28)

To evaluate the heading tracking effects of different controllers, the integral absolute errors (IAE) of the system is introduced as [38]

$$\text{IAE} = \int_0^{t_f} |\tilde{e}(t)| \text{d}t \tag{31}$$

where t_f is the simulation time, and $\tilde{e}(t)$ is the tracking error.

To design an NNI-MPHC for the wave glider, the related parameters values of three components MPC, NNI, and LRESO are given in Table 3, and the constraints of MPC are set as

$$-40° \le \delta_0(k) \le 40°, \quad -40° \le \Delta\delta_0(k) \le 40°$$

For comparison purpose, the existing heading controllers IADRC [10] and MADRC+IAW [11] are introduced, and the parametric values of components: tracking differentiator (TD), S-surface controller, and improved linear extended state observer (ILESO) (for IADRC), nonlinear state error feedback (NLSEF) controller, reduced-order extended state observer (RESO), and improved anti-windup (IAW) (for MADRC+IAW) are listed in Table 4.

Table 3. The parametric values of NNI-MPHC.

NNI-MPHC		
Component	**Parameter**	**Value**
MPC	Q	40
	R	0.27
	n	10
	m	3
	T	0.1
NNI	ρ	1.2
	λ	0.06
LRESO	β_{01}	26
	β_{02}	0.2
	b_0	0.1

Table 4. The parametric values of IADRC and MADRC+IAW.

IADRC [10]			MADRC+IAW [11]		
Component	**Parameter**	**Value**	**Component**	**Parameter**	**Value**
TD	r	1.2	TD	r	1.2
	h	1.0		h	1.0
S-surface	K_1	6.0	NLSEF	δ_0	0.25
controller	K_2	4.5	controller	α_P	0.5
	$K_{\max}$	40		α_D	1.5
ILESO	β_1	6.0		K_P	8.0
	β_2	12		K_D	0.5
	β_3	8.0	RESO	b_0	0.5
	K_f	0.2		δ	0.1
	α_f	0.7		β_1	0.01
	δ_f	1.5		β_2	20
	b_0	0.768		α_1	0.5
				α_2	0.25
			IAW	α	0.02
				η_p	0.2
				η_d	1

In particular, suppose that the NNI has already run for 200 s, and the identification result $\boldsymbol{V}(0)$ is set to

$$\boldsymbol{V}(0) = \begin{bmatrix} 0.015 & 0.639 & 0.045 & -1.051 & 0 & 0.020 \end{bmatrix}^T$$

4.2. Performance of Glider with Different Heading Controllers

In this section, with regard to the three cases listed in Table 2, using the NNI proposed in this paper, the identified system parameters a_{mn} and $b_m, m, n = 1, 2$ are obtained. As showed in Figures 6–8 for cases I–III, the designed online identification algorithm effectively estimates the system parameters of the wave glider.

Applying the designed heading controllers NNI-MPHC, IADRC [10], and MADRC+IAW [11] to the wave glider under aforementioned three different conditions, one calculates the yaw angle, tracking error, and speed of the wave glider. The corresponding curves are depicted in Figures 9–11, respectively, while the IAEs of the controlled wave glider are summarized in Tables 5–7 for cases I, II, and III, respectively. Additionally, it should be noted that in Figures 9 and 10, Tables 5 and 6, results of ideal condition are also provided.

Figure 9 and Table 5 demonstrate that even in the presence of external disturbance, the trajectory of wave glider with NNI-MPHC closely follows the ideal trajectory. From 0 to 200 s, the speed of the wave glider increases from a low value to a medium value. Thanks to the accurate parameter identification of NNI and the predictive optimization of MPC, the system avoids overshooting and ensures rapidity tracking performance. Although IADRC also exhibits good control performance, it lacks the same rapid response when the heading approaches the predefined signal. Meanwhile, the MADRC+IAW can prevent overshooting but does not guarantee ideal responsiveness.

As illustrated in Figure 10 and Table 6, the predictive capability of NNI-MPHC proves to have a crucial role again. Even in the presence of external disturbances, the controller effectively maintained both rapidity and accuracy in guiding the wave glider to track a time-varying target. Despite variations in speed at different times, NNI-MPHC consistently achieves the optimal control outcomes based on the identified model. In contrast, the heading controllers IADRC and MADRC+IAW suffer from the time delays in their TD, and the resulting heading control effects of the wave glider cannot reach the predefined input timely.

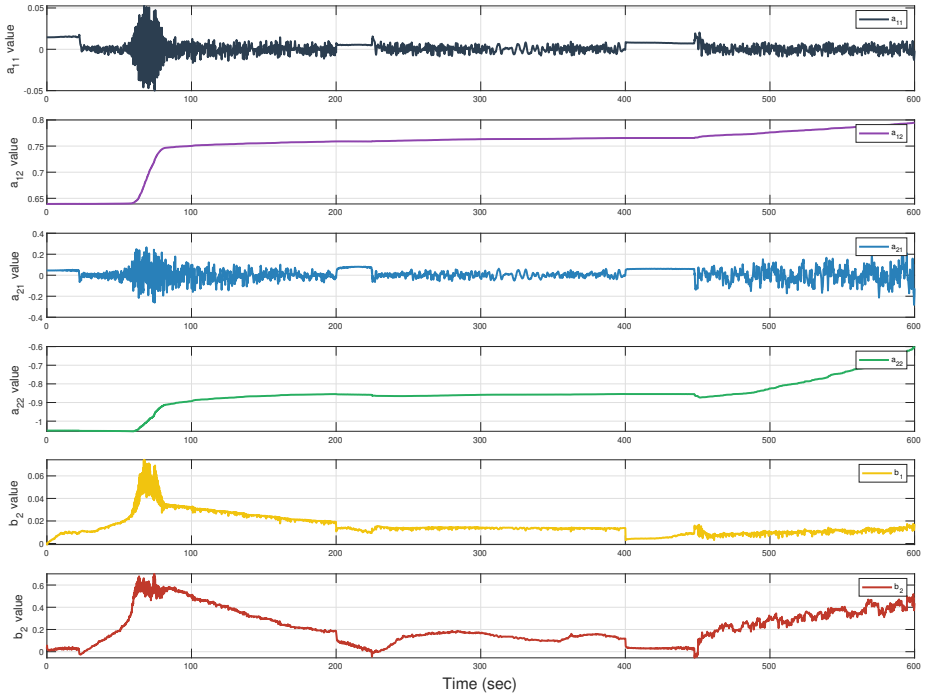

Figure 6. Case I—Identified systematic parameters versus time.

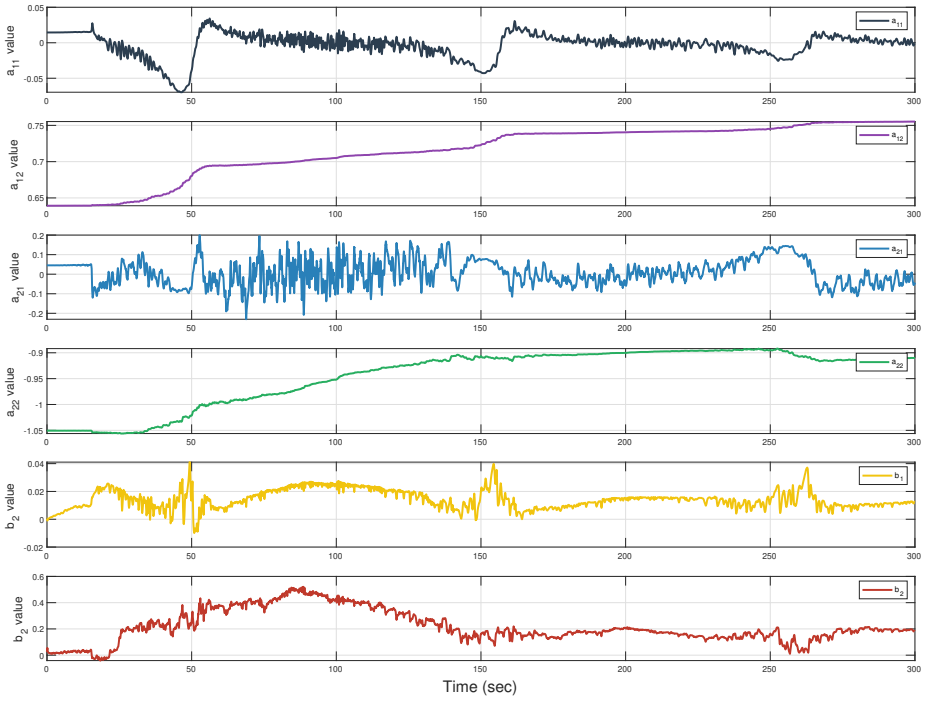

Figure 7. Case II—Identified systematic parameters versus time.

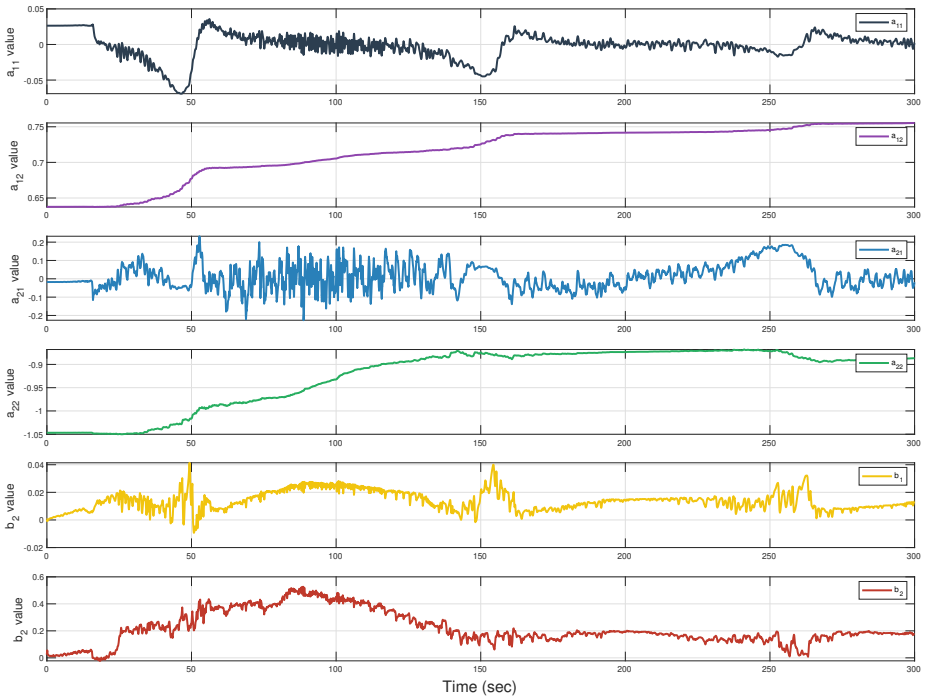

Figure 8. Case III—Identified systematic parameters versus time.

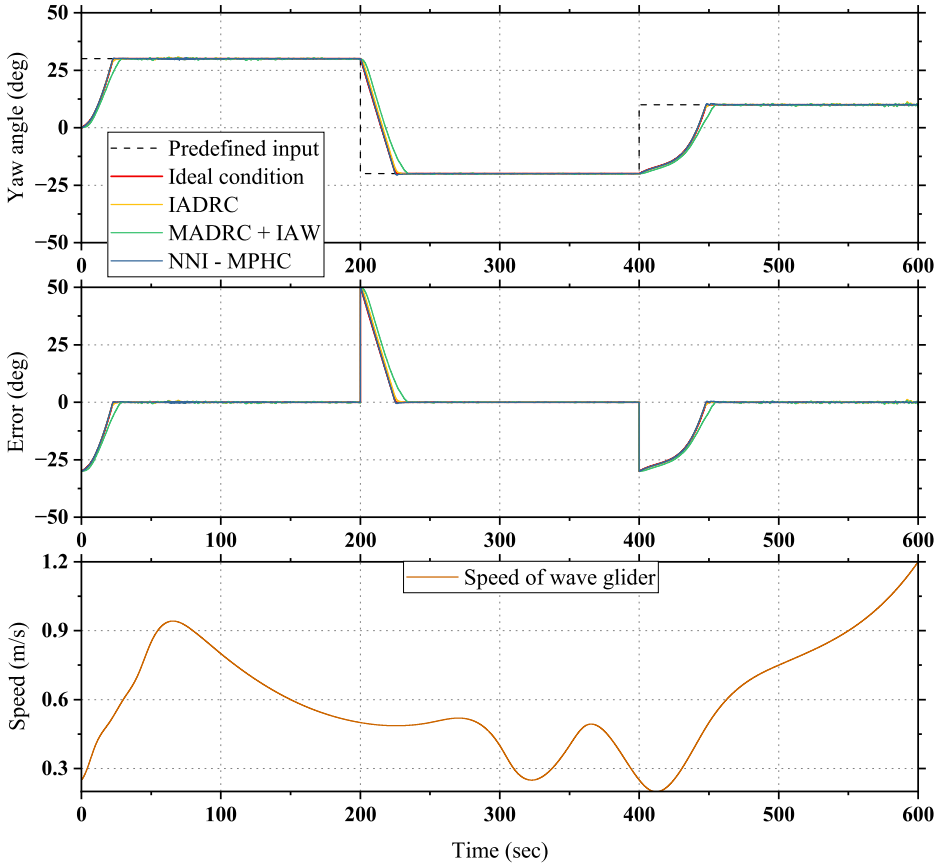

Figure 9. Case I—Yaw angle, tracking error, and speed of glider with different heading controllers.

Table 5. Case I—The IAEs of wave glider with different heading controllers.

Controller	t_f (s)	IAE (deg)
Ideal condition	600	2087.5
IADRC [10]	600	2203
MADRC+IAW [11]	600	2479
NNI-MPHC	600	2104.9

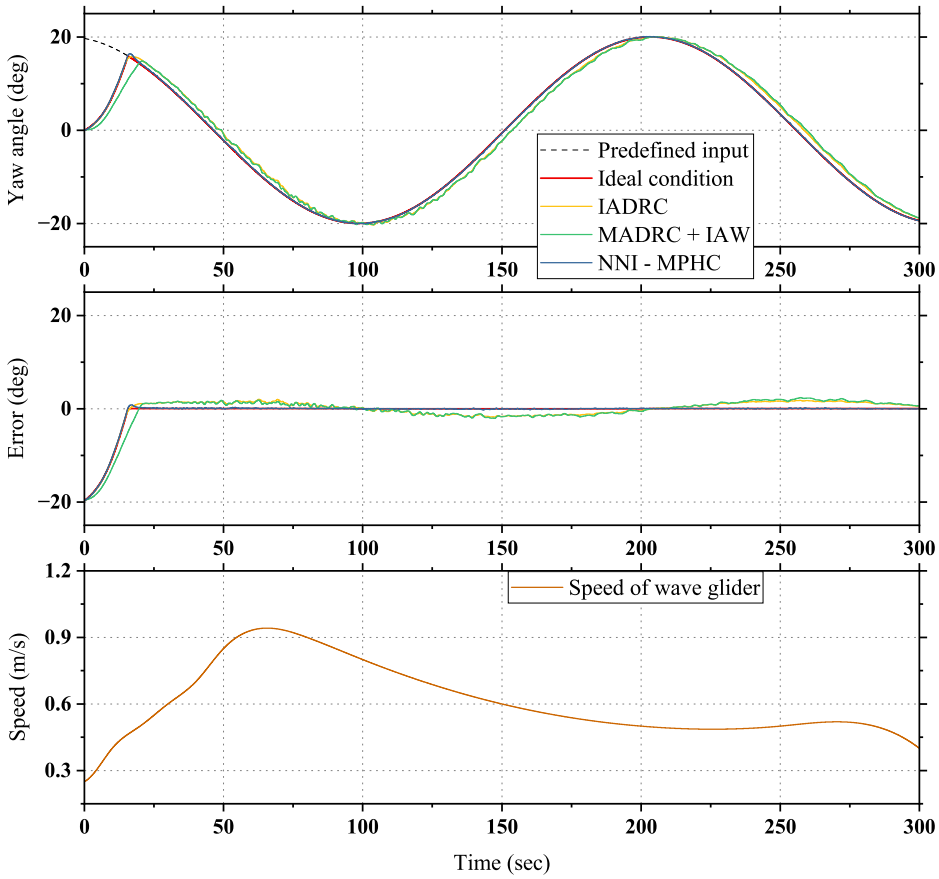

Figure 10. Case II—Yaw angle, tracking error, and speed of glider with different heading controllers.

Table 6. Case II—The IAEs of wave glider with different heading controllers.

Controller	t_f (s)	IAE (deg)
Ideal condition	300	193.0
IADRC [10]	300	504.0
MADRC+IAW [11]	300	556.0
NNI-MPHC	300	210.1

For case III, where the model uncertainty is taken into account, the heading control performance of the wave glider using NNI-MPHC remains almost identical to that in case II. However, the performance of system with IADRC and MADRC+IAW is significantly diminished. In fact, at listed in Tables 6 and 7, one can observe that the increase in IAE for the system with NNI-MPHC is smaller compared to that of IADRC and MADRC+IAW.

In summary, the proposed neural network identification-based model predictive heading control scheme effectively ensures the tracking performance of the wave glider. Additionally, the heading control not only improves tracking accuracy and responsiveness but also enhances the system robustness against external disturbance and model uncertainty.

These improvements make NNI-MPHC superior to most existing heading controllers for wave gliders.

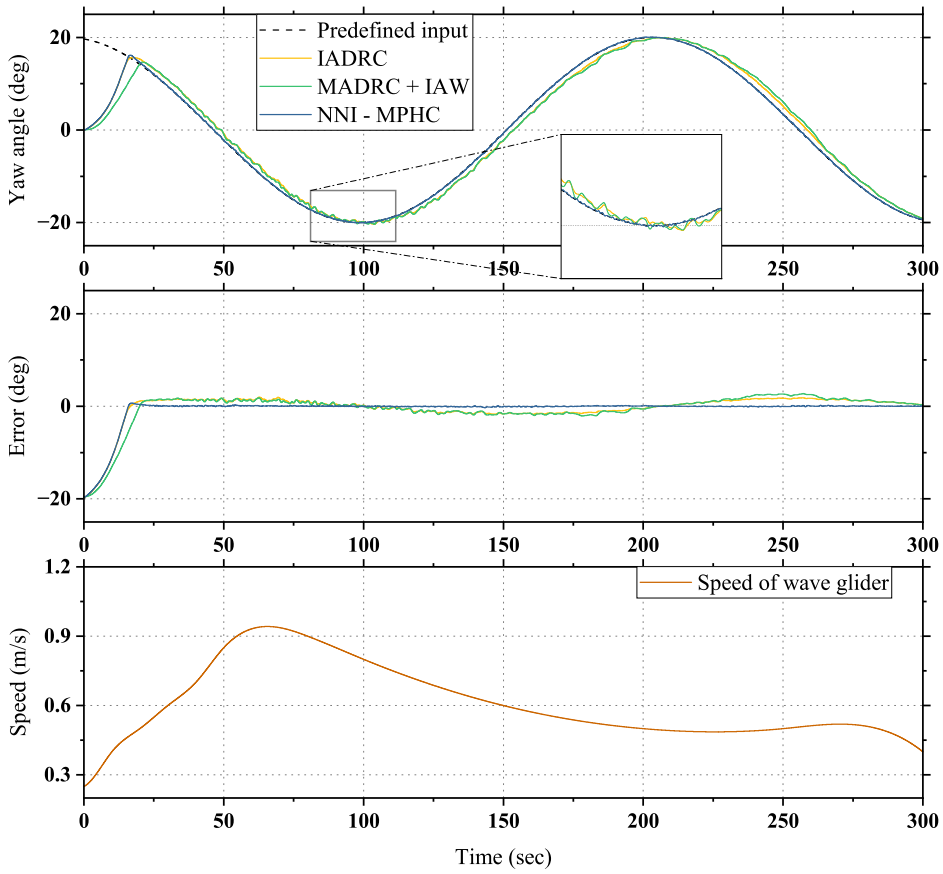

Figure 11. Case III − Yaw angle, tracking error, and speed of glider with different heading controllers.

Table 7. Case III − The IAEs of wave glider with different heading controllers.

Controller	t_f (s)	IAE (deg)
IADRC [10]	300	513.8
MADRC+IAW [11]	300	582.3
NNI-MPHC	300	217.1

5. Conclusions

In this paper, a neural network identification-based model predictive heading control scheme has been developed for the wave glider. The proposed heading controller consists of three key components: a model predictive controller, a neural network-based model identifier, and a linear reduced-order extended state observer. The algorithm for the MPC-based heading controller has been detailed, and simulation results have demonstrated the effectiveness and superiority of the proposed heading controller. It was found that the designed neural network identification-based model predictive heading controller significantly improves the steering performance of wave glider, offering rapid, accurate, and robust control.

However, several limitations of the proposed approach still exist: (i) The controller implemented in this study uses a basic MPC algorithm, which could be enhanced with more advanced predictive algorithms. (ii) The neural network could be upgraded to a more sophisticated architecture. (iii) The model used in this paper does not fully capture the specific characteristics of the wave glider, and this aspect could be refined in future iterations.

Several potential challenges remain in the heading control of wave glider. For instance, the development of a general double-body dynamic modeling and design of fixed-time heading controller are complex and require further investigation. In addition, given that the wave glider operates in a complex ocean environment, exploring network-based heading control and cooperative control of multi-wave-glider systems presents an interesting and promising direction for future research.

Author Contributions: Conceptualization, P.J.; Methodology, P.J.; Validation, P.J.; Formal analysis, Y.Z.; Data curation, P.J.; Writing—original draft, P.J.; Writing—review & editing, B.Z.; Supervision, B.Z.; Funding acquisition, B.Z. All authors have read and agreed to the published version of the manuscript.

Funding: This work was supported in part by the National Key R&D Program of China under Grant 2018AAA0100804.

Data Availability Statement: The data that support the findings of this study will be available from the corresponding author upon reasonable request.

Conflicts of Interest: The authors declare no personal, academic, or financial conflicts of interest associated with this paper.

References

1. Sun, X.; Zhou, Y.; Sang, H.; Yu, P.; Zhang, S. Adaptive path following control for Wave gliders in time-varying environment. *Ocean Eng.* **2020**, *218*, 108165. [CrossRef]
2. Yazdani, A.; MahmoudZadeh, S.; Yakimenko, O.; Wang, H. Perception-aware online trajectory generation for a prescribed manoeuvre of unmanned surface vehicle in cluttered unstructured environment. *Robot. Auton. Syst.* **2023**, *169*, 104508. [CrossRef]
3. Liu, F.; Liu, Y.; Sun, X.; Sang, H. A new multi-sensor hierarchical data fusion algorithm based on unscented Kalman filter for the attitude observation of the wave glider. *Appl. Ocean Res.* **2021**, *109*, 102562. [CrossRef]
4. Yazdani, A.; Sammut, K.; Yakimenko, O.; Lammas, A. A survey of underwater docking guidance systems. *Robot. Auton. Syst.* **2020**, *124*, 103382. [CrossRef]
5. Yazdani, A.; Sammut, K.; Yakimenko, O.; Lammas, A.; Tang, Y.; Mahmoud Zadeh, S. IDVD-based trajectory generator for autonomous underwater docking operations. *Robot. Auton. Syst.* **2017**, *92*, 12–29. [CrossRef]
6. Abbasi, A.; MahmoudZadeh, S.; Yazdani, A. A Cooperative Dynamic Task Assignment Framework for COTSBot AUVs. *IEEE Trans. Autom. Sci. Eng.* **2022**, *19*, 1163–1179. [CrossRef]
7. Wang, L.; Li, Y.; Liao, Y.; Pan, K.; Zhang, W. Course control of unmanned wave glider with heading information fusion. *IEEE Trans. Ind. Electron.* **2019**, *66*, 7997–8007. [CrossRef]
8. Yiming, L.; Ye, L.; Shuo, P. Variable-structure filtering method for an unmanned wave glider. *Appl. Ocean Res.* **2021**, *107*, 102450. [CrossRef]
9. Yiming, L.; Ye, L.; Shuo, P. Double-body coupled heading manoeuvrability response model considering umbilical lag of unmanned wave glider. *Appl. Ocean Res.* **2021**, *113*, 102640. [CrossRef]
10. Li, Y.; Pan, K.; Liao, Y.; Zhang, W.; Wang, L. Improved active disturbance rejection heading control for unmanned wave glider. *Appl. Ocean Res.* **2021**, *106*, 102438. [CrossRef]
11. Zhou, Y.; Sun, X.; Sang, H.; Yu, P. Robust dynamic heading tracking control for wave gliders. *Ocean Eng.* **2022**, *256*, 111510. [CrossRef]
12. Hu, Y.; Wang, H.; Yazdani, A.; Man, Z. Adaptive full order sliding mode control for electronic throttle valve system with fixed time convergence using extreme learning machine. *Neural Comput. Appl.* **2022**, *34*, 5241–5253. [CrossRef]
13. Chen, L.; Liu, J.; Wang, H.; Hu, Y.; Zheng, X.; Ye, M.; Zhang, J. Robust control of reaction wheel bicycle robot via adaptive integral terminal sliding mode. *Nonlinear Dyn.* **2021**, *104*, 2291–2302. [CrossRef]
14. Chen, L.; Zhang, H.; Wang, H.; Shao, K.; Wang, G.; Yazdani, A. Continuous adaptive fast terminal sliding mode-based speed regulation control of PMSM drive via improved super-twisting observer. *IEEE Trans. Ind. Electron.* **2023**, *71*, 5105–5115. [CrossRef]
15. Wen, H.; Li, X.; Liang, Z.; Yao, B.; Lian, L. Orientation control of the Wave Glider with uncertain environment disturbances and unknown variable hydrodynamics coefficients: Theory and simulation. *Ocean Eng.* **2023**, *275*, 114110. [CrossRef]
16. Wang, P.; Zhang, X.; Wang, D.; Guo, X.; Lu, W.; Tian, X. A restricted circle based position keeping strategy for the wave glider. *Appl. Ocean Res.* **2020**, *97*, 102081. [CrossRef]
17. Yu, P.; Sun, X.; Zhou, Y.; Sang, H.; Zhang, S. Adaptive station-keeping strategy for wave gliders considering uncertain environmental disturbances. *Ocean Eng.* **2023**, *277*, 114326. [CrossRef]
18. Zhang, S.; Sang, H.; Sun, X.; Liu, F.; Zhou, Y.; Yu, P. Research on the maneuverability and path following control of the wave glider with a propeller-rudder system. *Ocean Eng.* **2023**, *278*, 114346. [CrossRef]
19. Zhang, S.; Sang, H.; Sun, X.; Liu, F.; Zhou, Y.; Yu, P. A multi-objective path planning method for the wave glider in the complex marine environment. *Ocean Eng.* **2022**, *264*, 112481. [CrossRef]

20. Valencia-Palomo, G.; Rossiter, J.; López-Estrada, F. Improving the feed-forward compensator in predictive control for setpoint tracking. *ISA Trans.* **2014**, *53*, 755–766. [CrossRef]
21. Valencia-Palomo, G.; Rossiter, J. Novel programmable logic controller implementation of a predictive controller based on Laguerre functions and multiparametric solutions. *IET Control. Theory Appl.* **2012**, *6*, 1003–1014. [CrossRef]
22. Cui, D.; Zou, W.; Guo, J.; Xiang, Z. Neural network-based adaptive finite-time tracking control of switched nonlinear systems with time-varying delay. *Appl. Math. Comput.* **2022**, *428*, 127216. [CrossRef]
23. Atencia, M.; Joya, G.; Sandoval, F. Hopfield Neural Networks for Parametric Identification of Dynamical Systems. *Neural Process. Lett.* **2005**, *21*, 143–152. [CrossRef]
24. Yu, J.B.; Wu, Y.Q. Global robust tracking control for a class of cascaded nonlinear systems using a reduced-order extended state observer. *Nonlinear Dyn.* **2018**, *94*, 1277–1289. [CrossRef]
25. Kraus, N.D. Wave Glider Dynamic Modeling, Parameter Identification and Simulation. Master's Thesis, University of Hawaii at Manoa, Honolulu, HI, USA, 2012.
26. Wang, L.; Li, Y.; Liao, Y.; Pan, K.; Zhang, W. Dynamics modeling of an unmanned wave glider with flexible umbilical. *Ocean Eng.* **2019**, *180*, 267–278. [CrossRef]
27. Wang, P.; Tian, X.; Lu, W.; Hu, Z.; Luo, Y. Dynamic modeling and simulations of the wave glider. *Appl. Math. Model.* **2019**, *66*, 77–96. [CrossRef]
28. Wen, H.; Zhou, H.; Fu, J.; Zhang, X.; Yao, B.; Lian, L. Multi-body coupled dynamic modelling of the Wave Glider. *Ocean Eng.* **2022**, *257*, 111499. [CrossRef]
29. Fossen, T.I. *Handbook of Marine Craft Hydrodynamics and Motion Control*; John Wiley & Sons, Ltd.: Hoboken, NJ, USA, 2011; Chapter 7, pp. 133–186. [CrossRef]
30. Tsingtao Hydrotech Co., Ltd. Black Pearl Wave Glider. 2022. Available online: https://image.brandpano.com/app/cimee/2021pro/glider/index.html#/ (accessed on 6 December 2024).
31. Gu, N.; Wang, D.; Peng, Z.; Wang, J.; Han, Q.L. Disturbance observers and extended state observers for marine vehicles: A survey. *Control Eng. Pract.* **2022**, *123*, 105158. [CrossRef]
32. Habibi, H.; Yazdani, A.; Darouach, M.; Wang, H.; Fernando, T.; Howard, I. Observer-based sensor fault tolerant control with prescribed tracking performance for a class of nonlinear systems. *IEEE Trans. Autom. Control* **2023**, *68*, 8259–8266. [CrossRef]
33. Han, J. From PID to active disturbance rejection control. *IEEE Trans. Ind. Electron.* **2009**, *56*, 900–906. [CrossRef]
34. Cui, D.; Ahn, C.K.; Xiang, Z. Fault-Tolerant Fuzzy Observer-Based Fixed-Time Tracking Control for Nonlinear Switched Systems. *IEEE Trans. Fuzzy Syst.* **2023**, *31*, 4410–4420. [CrossRef]
35. Hopfield, J.J. Neurons with graded response have collective computational properties like those of two-state neurons. *Proc. Natl. Acad. Sci. USA* **1984**, *81*, 3088–3092. [CrossRef] [PubMed]
36. Maciejowski, J. *Predictive Control with Constraints*; Wiley Online Library: Hoboken, NJ, USA, 2003.
37. Li, Z.X. Research on Adaptive Heading Control of Wave Glider. Master's Thesis, Qingdao University of Science and Technology, Qingdao, China, 2022.
38. Schultz, W.C.; Rideout, V.C. Control system performance measures: Past, present, and future. *IRE Trans. Autom. Control* **1961**, *AC-6*, 22–35. [CrossRef]